

TRANSCRIPTOME ANALYSES REVEAL DIFFERENTIAL GENE EXPRESSION PATTERNS BETWEEN THE LIFE-CYCLE STAGES OF *EMILIANA HUXLEYI* (HAPTOPHYTA) AND REFLECT SPECIALIZATION TO DIFFERENT ECOLOGICAL NICHES¹

*Sebastian D. Rokitta*²

Alfred Wegener Institute for Polar and Marine Research, Am Handelshafen 12, 27570 Bremerhaven, Germany

Lennart J. de Nooijer

Department of Geosciences at Utrecht University, P.O. Box 80021, 3508 Utrecht, the Netherlands

Scarlett Trimborn

Alfred Wegener Institute for Polar and Marine Research, Am Handelshafen 12, 27570 Bremerhaven, Germany

Colomban de Vargas

CNRS, UMR7144 & Université Pierre et Marie Curie, Station Biologique de Roscoff, Équipe Eppo, Place George Teissier, 29680 Roscoff, France

Björn Rost and Uwe John

Alfred Wegener Institute for polar and marine research, Am Handelshafen 12, 27570 Bremerhaven, Germany

Coccolithophores, especially the abundant, cosmopolitan species *Emiliana huxleyi* (Lohmann) W. W. Hay et H. P. Mohler, are one of the main driving forces of the oceanic carbonate pump and contribute significantly to global carbon cycling, due to their ability to calcify. A recent study indicates that termination of diploid blooms by viral infection induces life-cycle transition, and speculation has arisen about the role of the haploid, noncalcifying stage in coccolithophore ecology. To explore gene expression patterns in both life-cycle stages, haploid and diploid cells of *E. huxleyi* (RCC 1217 and RCC 1216) were acclimated to limiting and saturating photon flux densities. Transcriptome analyses were performed to assess differential genomic expression related to different ploidy levels and acclimation light intensities. Analyses indicated that life-cycle stages exhibit different properties of regulating genome expression (e.g., pronounced gene activation and gene silencing in the diploid stage), proteome maintenance (e.g., increased turnover of proteins in the haploid stage), as well as metabolic processing (e.g., pronounced primary metabolism and motility in the haploid stage and calcification in the diploid stage). Furthermore, higher abundances of transcripts related to endocytotic and digestive machinery were observed in the diploid stage. A qualitative feeding experiment indicated that both life-cycle stages are capable of particle uptake (0.5 µm diameter) in late-stationary growth phase. Results showed

that the two life-cycle stages represent functionally distinct entities that are evolutionarily shaped to thrive in the environment they typically inhabit.

Key index words: endocytosis; life-cycle stages; microarray; quantitative RT-PCR; transcriptome profiling

Abbreviations: cRNA, complementary RNA; EMS, endomembraneous system; GPA, calcium binding protein with a high glutamic acid, proline, and alanine content; KOG, eukaryotic orthologous genes; PKS, polyketide synthase; qRT-PCR, quantitative real-time polymerase chain reaction

Phytoplankton are responsible for the majority of marine primary production and play an important role in the global cycling of biogenic elements (Falkowski and Raven 2007). As in all phytoplankton, the production of biomass results in the export of particulate organic carbon to depth (the so-called organic carbon pump). Coccolithophores further produce particulate inorganic carbon by precipitation of calcium carbonate. This process results in the removal of dissolved inorganic carbon from surface waters and sustains the vertical gradients of dissolved inorganic carbon and alkalinity in the oceans (Rost and Riebesell 2004). This phenomenon, known as the carbonate pump, is a critical component of the global carbon cycle that exerts a major influence on Earth's climate (Westbroek et al. 1993).

Coccolithophores are arguably the most productive group of calcifying organisms in today's oceans.

¹Received 17 May 2010. Accepted 14 January 2011.

²Author for correspondence: e-mail sebastian.rokitta@awi.de.

In particular, the morpho-species *E. huxleyi* accounts for 20%–50% of the total coccolithophore community in most areas and close to 100% in subpolar waters (Winter et al. 1994, Mohan et al. 2008). In contrast to most other coccolithophore species, it can form massive blooms, often related to the annual spring succession. While the initiation of *E. huxleyi* blooms appears to be controlled in a bottom-up manner (e.g., by nutrient availability, irradiance, or stratification), their termination by viruses is a clear example of top-down regulation in plankton ecology (Bratbak et al. 1996, Schroeder et al. 2003). Frada et al. (2008) suggested that virus-mediated termination of diploid populations induces a meiotic transition in some individuals followed by the growth of a new haploid population. This transition was termed the “Cheshire Cat” escape strategy, by which *E. huxleyi* seeks refuge in its haploid, apparently virus-resistant life-cycle stage.

Coccolithophores in general are known to follow a haplo-diplontic life cycle, with individuals of both stages being able to propagate independently by mitosis (Billard 1994). *E. huxleyi* can exist in a coccolith-bearing form, which is diploid (2N, i.e., possessing the double set of chromosomes) and in a noncalcifying flagellated form with organic scales that is haploid (1N, i.e., possessing the reduced, single set of chromosomes). A third form, known to be diploid, nonmotile, and uncalcified, may be a culture artifact (Klaveness 1972, Green et al. 1996). Until recently, coccolithophore research has largely ignored the haploid life-cycle stage of *E. huxleyi* due to the absence of calcification and assumed limited biogeochemical impact. The haploid cells, however, apparently immune to viral attacks, are not obliged to undergo sexual fusion. Thus, they may persist independently in nature for long periods of time and form new inocula for diploid offspring populations after spatial and/or temporal dispersion (Frada et al. 2008). Regarding this important ecological role, the two stages are likely to represent differentiated entities that are evolutionarily shaped to fulfill their ecological purpose in the contrasting environments they typically occupy. Furthermore, the obvious morphological differences between the two stages (flagellae in 1N, calcification in 2N) suggest significantly divergent physiologies a priori, for example, regarding carbon/nutrient uptake mechanisms, energy budgeting, and/or trophic modes of biomass acquisition (i.e., phagotrophy).

Phagotrophy involves endocytosis, a main constitutive function of the endomembrane system (EMS). EMS-derived organelles can be selectively equipped with protein/enzymatic machinery, enabling cells to establish a variety of chemical microenvironments within, for example, for digestion or calcification (Corstjens and Gonz ales 2004). Anterograde (outward) traffic lines of the EMS deliver membrane material, receptors, and enzymes to the plasma membrane or the extracellular space by

fusing vesicles to the plasma membrane (exocytosis). Vice versa, the retrograde traffic lines retrieve recyclable protein material and membrane material by internalization and constriction (endocytosis) and can also serve to take up material from the extracellular space for trophic purposes (i.e., phagotrophy). Especially in protists, phagotrophy plays a key role, as it provided (and still provides) a prerequisite for heterotrophic feeding and the evolution of photoautotrophy in eukaryotes (Raven 1997). Mixotrophy, for example, has been observed in numerous haptophytes (Jones et al. 1994) and was also suspected for *E. huxleyi* (Houdan et al. 2005).

Furthermore, the difference in DNA content between the life-cycle stages necessitates regulatory activities to control stage-specific expression of genes. Cellular gene regulation is versatile and can be applied on the levels of DNA (e.g., condensation or decondensation of chromosomes), RNA (e.g., posttranscriptional and translational regulation), or protein (e.g., posttranslational modifications). Hence, the level the regulation is applied on has different implications regarding the cell’s energetic effort and ecological benefits (e.g., response times to external stimuli). To understand the differences between the life-cycle stages, a deeper understanding of the regulation of gene expression (i.e., the usage of the respective genomes) is crucial.

In this study, the differential gene expression patterns between high- and low-light-acclimated haploid (uncalcified) and diploid (coccolith bearing) life-cycle stages of *E. huxleyi* (RCC 1217 and RCC 1216) were assessed. As analyses yielded evidence for increased endocytotic and proteolytic activity in silico, preliminary follow-up feeding experiments were performed with both life-cycle stages.

MATERIALS AND METHODS

Culture conditions. Axenic haploid and diploid cells (strains RCC 1217 and RCC 1216, respectively, obtained from the Roscoff culture collection) of *E. huxleyi* were grown as dilute-batch cultures at 15°C in 0.2 µm filtered modified F/2 medium, consisting of North Sea water (salinity 32.2 psu), enriched with vitamins and trace metals (Guillard and Ryther 1962). Nitrate and phosphate were added to concentrations of 100 and 6.25 µM, respectively. Cultures were exposed to light intensities of 50 and 300 µmol photons · m⁻² · s⁻¹ provided by Biolux 965 daylight lamps (Osram, M unchen, Germany) at a 16:8 light:dark cycle. Light intensities were adjusted using a LI-1400 datalogger (Li-Cor, Lincoln, NE, USA) with a 4π-sensor (Walz, Effeltrich, Germany). Cells were acclimated to culture conditions for at least 2 weeks prior to sampling. Cylindrical flasks of 900 mL were continuously bubbled through a frit with humidified ambient air (130 ± 10 mL · min⁻¹) to avoid cell sedimentation. Cell concentrations were monitored using a Multisizer III hemocytometer (Beckman-Coulter, Fullerton, CA, USA). The pH was monitored daily using a pH3000 microprocessor pH-meter (WTW, Weilheim, Germany), which was calibrated using National Institute of Standards and Technology-certified buffer systems (therefore referred to as pH_{NBS}). Culture pH_{NBS} did not deviate more than 0.05 units from cell-free medium.

TABLE 1. Carbonate chemistry, growth rates, and cellular quotas of particulate organic carbon/inorganic carbon (POC, PIC).

Culture	pH _{NBS}	Dissolved inorganic carbon ($\mu\text{mol} \cdot \text{kg}^{-1}$)	Total alkalinity ($\mu\text{mol} \cdot \text{kg}^{-1}$)	$f\text{CO}_2$ (μatm)	Growth (μ) (d^{-1})	POC ($\text{pg} \cdot \text{cell}^{-1}$)	PIC ($\text{pg} \cdot \text{cell}^{-1}$)
1N LL	8.176 \pm 0.005	2,111 \pm 19	2,393 \pm 24	351 \pm 7	0.87 \pm 0.12	7.7 \pm 0.7	0.6 \pm 0.1
1N HL	8.177 \pm 0.019	2,096 \pm 24	2,380 \pm 10	350 \pm 4	1.18 \pm 0.20	9.7 \pm 1.9	0.6 \pm 0.4
2N LL	8.112 \pm 0.014	1,997 \pm 44	2,254 \pm 20	399 \pm 4	0.63 \pm 0.14	7.5 \pm 0.5	10.4 \pm 0.6
2N HL	8.083 \pm 0.004	2,018 \pm 15	2,273 \pm 5	430 \pm 2	1.02 \pm 0.15	10.8 \pm 1.4	8.8 \pm 2.3
Reference	8.134 \pm 0.010	2,134 \pm 25	2,411 \pm 13	404 \pm 12	–	–	–

HL, high light; LL, low light.

Cells were harvested during the exponential growth phase, at average cell concentrations of 90,000 cells \cdot mL⁻¹, to avoid effects of shifted carbonate chemistry (Table 1). Calculations of the carbonate system were based on measurements of pH_{NBS}, total alkalinity, temperature, and salinity and were performed with the program CO₂sys (Lewis and Wallace 1998). For the calculations, average phosphate concentrations of 4 μ M were assumed. Dissociation constants of carbonic acid (Mehrbach et al. 1973 refit by Dickson and Millero 1987) and the dissociation constants of sulfuric acid (Dickson 1990) were used. Results are reported for 15°C. Samples were taken between 4 and 8 h after the start of the light period.

RNA sampling. Samples of $\sim 1.5 \times 10^7$ cells were concentrated by filtration (1.2 μ m polycarbonate filters; Millipore, Billerica, MA, USA) and pelleted by 5 min centrifugation at 5,000g in a table centrifuge (Hettich, Bäch, Switzerland). Cell disruption was performed with a beadmill (Qiagen, Hilden, Germany) after adding 100 μ L glassbeads (0.1 mm). Lysate was homogenized using QIAshredder spin-columns (Qiagen). RNA extraction was performed using a silica-column-based guanidinium thiocyanate method (RNeasy mini; Qiagen). To digest DNA in the isolate, 7 Kunitz units of bovine DNase I (Qiagen) were applied to the silica matrix following incubation for 20 min at room temperature. After elution, MicroCon YM 30 ultrafiltration columns (Millipore) were used to further enrich RNA. Concentration and purity were measured photometrically with a Nanodrop ND1000 (PepLab, Erlangen, Germany), and integrity of the isolate was assessed using a BioAnalyzer 2100 (Agilent, Santa Clara, CA, USA) running an RNA 6000 Nano LabChip (Agilent).

Microarray hybridizations. RNA Spike-In Mix (Agilent, p/n 5188-5279) was added to the RNA samples prior to the labeling reactions serving as internal standard and benchmark for hybridization performance (Agilent RNA Spike-In Kit protocol). Two hundred nanograms total RNA was reversely transcribed, amplified, and labeled using the two-color low RNA Input fluorescent linear amplification kit (Agilent, p/n 5184-3523). Incorporation of Cy-3 and Cy-5 labeled cytidine 5'-triphosphate (Perkin Elmer, Waltham, MA, USA) was verified photometrically using the NanoDrop ND1000 (PepLab). Labeling efficiencies were calculated as pmol dye \cdot (ng cRNA)⁻¹ from the results of photometry and were in the range of 0.013–0.018 pmol dye \cdot (ng cRNA)⁻¹. Individual microarray hybridizations were carried out in biological triplicates according to the scheme presented in Figure 1 using SureHyb hybridization chambers (Agilent, p/n G2534A). Seven hundred fifty nanograms of each Cy-3 and Cy-5 labeled cRNA was hybridized to 4 \times 44K *E. huxleyi* custom-built microarrays (Agilent), containing 60mer oligonucleotide probes. Microarray probes were derived from computer-predicted “best gene models” compiled from the *E. huxleyi* CCMP1516 genome project, conducted by the U.S. Department of Energy Joint Genome Institute (JGI; <http://www.jgi.doe.gov>) in collaboration with the user community. Probe design was done using Agilent’s eArray online platform. Following the Two-Color

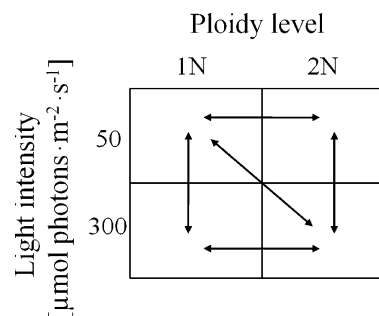


FIG. 1. Hybridization scheme of microarray experiments to test the effect of acclimation light intensity and ploidy levels on *Emiliania huxleyi*; vertical hybridizations report irradiance effects on either haploid or diploid gene expression. Horizontal hybridizations reveal ploidy-level effects on low- and high-light-acclimated cultures. The diagonal cross hybridization reports cumulative ploidy- and irradiance-related effects. These can be superimposed on the acquired data set and reduce the significant features to a more feasible number.

Microarray-based Gene Expression Analysis protocol (Agilent, p/n 5188-5242), hybridization was performed in a hybridization oven at 65°C for 17 h at an agitation of 6 rpm. After hybridization, microarrays were disassembled in Wash Buffer 1 (Agilent, p/n 5188-5325), washed with Wash Buffer 1, Wash Buffer 2 (Agilent, p/n 5188-5326), acetonitrile (VWR, Darmstadt, Germany), and Stabilization and Drying Solution (Agilent, p/n 5185-5979) according to manufacturer’s instructions. Stabilization and Drying Solution, an ozone scavenger, protects the Cy-dye signal from degradation. Arrays were scanned with a G2565BA microarray scanner (Agilent) using standard photomultiplier tube settings and 5 μ m scan resolution.

Microarray data evaluation. Raw data were extracted with Feature Extraction Software version 9.0 (Agilent), incorporating the GE2_105_Dec08 protocol. Array quality was monitored using the QC Tool v1.0 (Agilent) with the metric set GE2_QCMT_Feb07. Spots that had been flagged “outliers,” “not known,” or “bad” based on background median analysis were excluded from further processing. The data set was automatically normalized by the Feature Extraction Software using the locally weighted scatterplot smoothing (LOWESS) algorithm. Normalized data were submitted to the MIAMEexpress database hosted by the European Bioinformatics Institute (EBI; <http://www.ebi.ac.uk/arrayexpress>; accession code E-MEXP-2896). Gene expression analysis was performed using the MultiExperiment Viewer 4.2 (MEV), which is part of the TM4 Software suite (Saeed et al. 2003). Triplicate experiments were statistically evaluated in single class tests using the “significance analysis of microarrays” (SAM) algorithm introduced by Tusher et al. (2001). Data sets were permuted 500 times each, and differential gene expression was called significant when gene-specific *q*-values, which represent a statistically estimated

false discovery rate (Storey 2003), were $\leq 0.1\%$. Significant array features were assigned to “best gene model” predictions using available classifications of eukaryotic orthologous genes (KOG), provided by the JGI. Acquired KOG-based data sets were visually inspected toward key enzymes or expression patterns that may give hints to underlying metabolic pathways or cytobiological processes being more prominent in either the haploid or diploid stage. In the following, exemplary transcripts will be notated with their associated JGI Protein ID#.

Quantitative real-time polymerase chain reaction (qRT-PCR) validation. Primer sets for qRT-PCR were designed with PrimerExpress software 2.0.0 (Applied Biosystems, Darmstadt, Germany) for seven genes of interest after the visual inspection of the microarray data set (Table S1 in the supplementary material). Total RNA (250 ng) of haploid and diploid cultures was spiked with known concentrations of transcripts of the “nitrile-specifier protein” (NSP; 10 pg) and “major allergen” (MA; 10 ng) genes from the cabbage butterfly *Pieris rapae*. These “alien spikes” were used for the relative quantification using the $2^{-\Delta\Delta C_t}$ method (Livak and Schmittgen 2001) and served as a control for pipetting error as well as performance and linearity of cDNA synthesis (Krell et al. 2007). Spiked RNA was submitted to linear reverse transcription using SuperScript III reverse transcriptase (Invitrogen, Carlsbad, CA, USA) and anchored poly-dT Primers (Invitrogen). Resulting first strand cDNA was diluted and 2.5 ng of cDNA were amplified in a quantitative reverse transcription using Sybr Green I reporter dye master mix (Applied Biosystems, Foster City, CA, USA) and a Prism 7000 qRT-PCR cycler (Applied Biosystems) to measure relative expression of transcripts. Efficiencies of qRT-PCR primer sets were assessed by amplifying serial dilutions of generated cDNA. Curves were used to calculate the fold change of transcript expression relative to the haploid stage grown under low light (1N LL). Absolute target-copy-number calibrations for AP2B1 and ATPVa were performed by amplifying dilution series of known concentrations of DNA amplicons generated by PCR. The PCR primers for these quantifications were generated with Primer3 (Rozen and Skaletsky 2000; Table S1).

Microbead cell treatment. To test for endocytotic capacities, 1N and 2N cultures were grown under $40 \mu\text{mol photons} \cdot \text{m}^{-2} \cdot \text{s}^{-1}$ in 50 mL culture flasks. Ten milliliter subsamples were taken at different time points during the phases of culture

growth and incubated with sulfate-coated fluorescent beads (Sigma-Aldrich, Hamburg, Germany) of $0.5 \mu\text{m}$ diameter with a final concentration of $15\text{--}20 \text{ beads} \cdot \text{cell}^{-1}$. Cultures were spiked with $100 \mu\text{L}$ of dissolved organic matter 16 h prior to incubation with the fluorescent microspheres because additions of organic compounds have been shown to stimulate possible phagotrophic activity in phytoplankton (Legrand and Carlsson 1998). The added dissolved organic matter consisted of sterile-filtered ($0.2 \mu\text{m}$) beadmill-lysate of $\sim 2.5 \times 10^7$ *E. huxleyi* cells resuspended in 2 mL medium. After 60 min of incubation with the beads, cells were fixed with formaldehyde to an effective concentration of 5% (v/v). Cells were then scanned using a confocal laser-scanning microscope (Leica TCS, Wetzlar, Germany) that allowed separate detection of both the microspheres (excitation at 488 nm; detection at 500–560 nm) and chl *a* (excitation at 488 nm; detection at 610–670 nm) from single cells. Fluorescent scans were combined with bright field images to locate the chloroplasts and the microspheres within the cells.

RESULTS

Gene expression analysis. Hybridization data reported no significant transcriptomic differences between high-light and low-light acclimations in either haploid or diploid cultures (Fig. 2a). Cross-hybridizations (Fig. 1, diagonal arrow; 2a, dashed circle), representing expression patterns in response to different light acclimations and ploidy stages, indicated strong expression regulation ($>6,700$ significant features), but only very few of them (<10) were differentially expressed as a response originating from different acclimation light intensities.

In contrast, 1,840 and 2,449 features were determined to be expressed significantly higher and lower in diploid individuals (i.e., correspondingly lower and higher expressed in haploid individuals) under both light intensities, indicating distinct patterns of gene expression originating from different life-cycle stages (Fig. 2b). Cross-hybridizations (Fig. 2b, dashed circle) strongly supported this

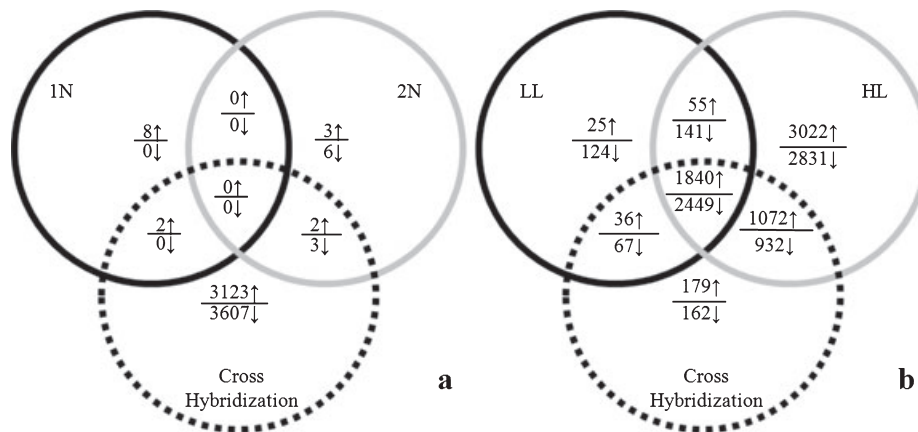


FIG. 2. (a) *Emiliania huxleyi* transcriptomic responses to different acclimation light intensities of the haploid (1N, black circle) and diploid (2N, gray circle) cells. Dashed circle represents cross hybridization; \uparrow = up-regulated in high light, \downarrow = down-regulated in high light. Central intersection holds the transcriptomic effect exclusively related to acclimation light intensity. (b) Transcriptomic responses to changes in ploidy level in low-light-acclimated (LL, black circle) and high-light-acclimated (HL, gray circle) cells. Dashed circle represents cross hybridization; \uparrow = up-regulated in the diploid transcriptome, \downarrow = down-regulated in diploid transcriptome. Central intersection holds the transcriptomic effect exclusively linked to differences in ploidy level.

conclusion, as they shared 95.6% of the significant features within the common intersection of ploidy responses in both light treatments. After assigning significant features to KOG annotations derived from gene models, a de visu evaluation of the obtained data set confirmed differential expression of various cellular functions between the two life-cycle stages (Table 2; and see Table S2 in the supplementary material for details).

In the following section, increased relative abundances of gene transcripts in the different stages are reported, meaning that these transcripts contribute to a higher extent to the respective stage-specific transcriptome. As expression ratios were assessed, it is important to note that presence of respective transcripts in the other stage is not excluded. However, the relative compositions of the transcriptomes differ clearly between stages.

Haplont-specific transcriptome features. In the haploid stage of *E. huxleyi*, increased relative expression

TABLE 2. Significantly up-regulated transcriptome features in diploid (2N) and haploid (1N) *Emiliania huxleyi*, classified by eukaryotic gene orthologies (KOG).

KOG classification of models	2N ↑	1N ↑
1. Amino acid transport and metabolism	19	28
2. Carbohydrate transport and metabolism	23	24
3. Cell cycle control, cell division, chromosome partitioning	4	8
4. Cell wall/membrane/envelope biogenesis	7	8
5. Chromatin structure and dynamics	18	6
6. Coenzyme transport and metabolism	0	8
7. Cytoskeleton and cell motility	40	101
8. Defense mechanisms	3	3
9. Energy production and conversion	20	27
10. Extracellular structures	23	18
11. Function unknown	30	43
12. General function prediction only	114	82
13. Inorganic ion transport and metabolism	28	20
14. Intracellular trafficking, secretion, and vesicular transport	10	17
15. Lipid transport and metabolism	9	20
16. Nuclear structure	1	5
17. Nucleotide transport and metabolism	0	6
18. Posttranslational modification, protein turnover, chaperones	35	47
19. Replication, recombination, and repair	5	14
20. RNA processing and modification	28	10
21. Secondary metabolite biosynthesis, transport, and catabolism	7	13
22. Signal transduction mechanisms	77	72
23. Transcription	48	44
24. Translation, ribosomal structure, and biogenesis	20	9
25. No functional annotation data available	1,273	1,816
Total	1,840	2,449

of nitrogen-distributing enzymes, such as aspartate aminotransferase (JGI# 413787), glutamine synthetase (JGI# 69253), glutaminase (JGI# 68199), threonine/serine dehydratase (JGI# 417175), and urea transporters (JGI# 194219), was observed (amino acid transport and metabolism; KOG class 1).

The relative expression levels of genes related to coenzyme transport and metabolism (KOG class 6) were also significantly higher in the haploid stage. Detected features include enzymes involved in synthesis of cobalamin derivatives (cobalamin-synthesis protein; JGI# 456427) and folic acid (methylenetetrahydrofolate dehydrogenase; JGI# 448747).

The haploid stage further intensively expressed cytoskeletal intermediary filaments like tubulins α (JGI# 445562) and β (TubB; JGI# 464996) and associated motor machinery, that is, subunits of dyneins (DynH, JGI# 75572) and kinesins (Kin, JGI# 101580; KOG class 7).

Higher relative abundances of transcripts coding for genes involved in carbon metabolism (isocitrate lyase; JGI# 436528), the tricarboxylic acid cycle (malate dehydrogenase; JGI# 414497), and general energy metabolism (pyruvate carboxylase, JGI# 456927; F₀F₁-ATP-Synthase subunits, JGI# 441432) were detected (KOG class 9).

The Ca²⁺-binding protein GPA (JGI# 431830), which is usually attributed to calcification (Corstjens et al. 1998, Schroeder et al. 2005), was found to be more prominently expressed in the haploid stage (KOG class 12).

Finally, features related to posttranslational modifications (KOG class 18) were also more strongly expressed in haploid *E. huxleyi*: Higher abundances of transcripts related to ubiquitin-mediated proteasomal degradation (e.g., E3 ubiquitin ligase, E3UL, JGI# 106507) as well as 26S proteasome compounds and the associated regulatory proteins (e.g., JGI# 449934) were observed.

Diplont-specific transcriptome features. The diploid stage exhibited increased expression of machinery involved in chromatin structuring and dynamics (KOG class 5). Numerous transcripts of genes participating in nucleosome remodeling (POB3 homologs, JGI# 451523), gene activation (histone-acetyltransferase, JGI# 365731), and gene silencing (histone H3 [Lysine-9] methyltransferase; JGI# 450763) were detected to be prominently expressed.

Transcripts of polyketide synthases (PKSs; JGI# 631889 and 631892; KOG class 8) were found in the diploid data set.

Features related to energy production and conversion (KOG class 9) indicated prominent expression of various subunits of a vacuolar H⁺-ATPase (V-ATPase, e.g., subunit α , JGI# 439538).

Regarding the transport of inorganic ions (KOG class 13), the Ca²⁺/H⁺ antiporter CAX3 (JGI# 416800) and a Na⁺-independent Cl⁻/HCO₃⁻ exchanger (AE, JGI# 99943) were expressed in the calcifying diploid stage.

Furthermore, transcript abundances related to vesicular traffic (KOG class 14) were generally higher in the diploid stage, the data set revealing prominent presence of clathrin-coated vesicle-related machinery (adaptor protein 2 subunit β_1 , AP2B1, JGI# 558382) and vacuolar protein sorting factors of the SNARE-type (JGI# 465386).

Increased expression of genes related to post-translational modifications (KOG class 18) was also found. A set of various vacuolar peptidases, for example, subtilisin-related vacuolar protease B (SVP1, JGI# 436633) and aspartyl-, asparaginyl-, and metallopeptidases (JGI# 112299, 455379, 451158) was prominently expressed in the diploid stage.

Features relevant for RNA processing and modification (KOG class 20) indicated elevated abundance of splicing coactivators of the so-called SR family (JGI# 427170), which are components of small nuclear ribonucleoproteins (snRNPs) and also of proteins acting in pretranslational RNA processing (RNA helicase, JGI# 418728) in the diploid cells.

qRT-PCR validation. To validate the microarray results, the expression levels of seven genes of interest were assessed by means of qRT-PCR (Table 3). Results were normalized to the abundance levels detected in haploid, low-light-acclimated cultures (1N LL) and are given in relative fold change. The assessed abundances agree with the outcome of the statistical microarray evaluation.

Two transcripts important for clathrin-mediated endocytosis (AP2B1, JGI# 558382) as well as for vacuolar acidification (ATPVa, JGI# 439538) were quantified absolutely (Fig. 3), showing that AP2B1 transcripts were expressed in the haploid stage of *E. huxleyi* ($0.71\text{--}1.06 \times 10^5$ copies \cdot [ng cDNA] $^{-1}$), but their abundance in the diploid stage ($3.5\text{--}5.3 \times 10^5$ copies \cdot [ng cDNA] $^{-1}$) was 3- to 5-fold higher. With respect to light intensities, obtained means of transcript copy numbers were proved not significantly different in both life-cycle stages (*t*-test, $P = 0.05$). Transcript abundances of the V-ATPase alpha subunit were >1,000-fold higher in the diploid cells ($11.8\text{--}13.0 \times 10^6$ copies \cdot [ng cDNA] $^{-1}$) compared to the haploid cells ($4.7\text{--}11.1 \times 10^3$ copies \cdot [ng cDNA] $^{-1}$). Effects of light intensity on expression levels could not be confirmed, the means of the light treatments were only insignificantly different (*t*-test, $P = 0.05$) in both stages.

Microbead cell treatment. The presence of gene transcripts related to clathrin-coated vesicles and

degradative machinery was shown by both microarray (Table 2; Table S2) and qRT-PCR (Table 3).

Preliminary feeding experiments indicated that both life-cycle stages are capable of endocytotic uptake of particles: While no bead ingestion could be detected during exponential and initial stationary growth phase, endocytosed particles could be observed in the last sampling, 2–3 d after entering stationary phase (Fig. 4). Fluorescence microscopy observations revealed that within an incubation time of 1 h up to 8 beads \cdot cell $^{-1}$ were taken up in both haploid and diploid individuals. Beads were typically observed to reside in the center of the cells, between the two chloroplasts (Fig. 5).

DISCUSSION

Microarray analyses revealed that overall *E. huxleyi* expression patterns, as obtained with the applied test sharpness, were not detectably altered by the different acclimation light intensities. The KOG database used contained only few genes related to photosynthesis, but this cannot account for the small absolute amount of significant features (Fig. 2a). Alterations in light intensity of this order of magnitude ($50\text{--}300 \mu\text{mol photons} \cdot \text{m}^{-2} \cdot \text{s}^{-1}$) resemble short-term variations typically imposed in nature (e.g., by cloud shading or vertical mixing). Hence, the transcriptomic indifference may be attributed to the ability of *E. huxleyi* to cope with such variability in irradiances at the photophysiological or posttranslational level rather than on the transcriptional level. In contrast, clear ploidy-dependent regulation patterns were observed (cf. Table 2; Table S1).

Haplont-specific transcriptome. A prominent relative increase in the expression of genes involved in nitrogen metabolism was detected in haploid *E. huxleyi*, including glutamine synthetase, the entry enzyme for ammonia into the metabolism. Furthermore, increased expression of multispecific aminotransferases as well as serine/threonine dehydratase suggests a close connection between the amino acid and carboxylic acid metabolism.

Transcripts of vitamin-synthesizing enzymes were prominent in the haploid stage of *E. huxleyi*. The diploid stage of at least one strain of *Emiliania* was determined to lack the ability to synthesize thiamine and cobalamin (Provasoli and Carlucci 1974). Consequently, as the organism obviously possesses the

TABLE 3. Quantitative real-time polymerase chain reaction (qRT-PCR) validations of seven transcripts.

	AP2B1	ATPVa	DynH	Kin	TubB	E3UL	SVP1
1N LL	1.0 \pm 0.2	1.0 \pm 0.3	1.0 \pm 0.3	1.0 \pm 0.1	1.0 \pm 0.2	1.0 \pm 0.2	1.3 \pm 1.2
1N HL	0.7 \pm 0.1	2.6 \pm 2.2	1.1 \pm 0.5	0.8 \pm 0.1	1.0 \pm 0.3	1.7 \pm 0.6	4.3 \pm 2.1
2N LL	4.4 \pm 1.7	4,052 \pm 1,094	0.25 \pm 0.1	0.003 \pm 0.001	0.1 \pm 0.1	0.1 \pm 0.04	773.0 \pm 293
2N HL	2.8 \pm 0.8	3,624 \pm 896	0.14 \pm 0.04	0.004 \pm 0.001	0.1 \pm 0.04	0.1 \pm 0.04	632.4 \pm 502

HL, high light; LL, low light.

Values indicate fold change in relation to haploid low-light-acclimated cells (1N LL).

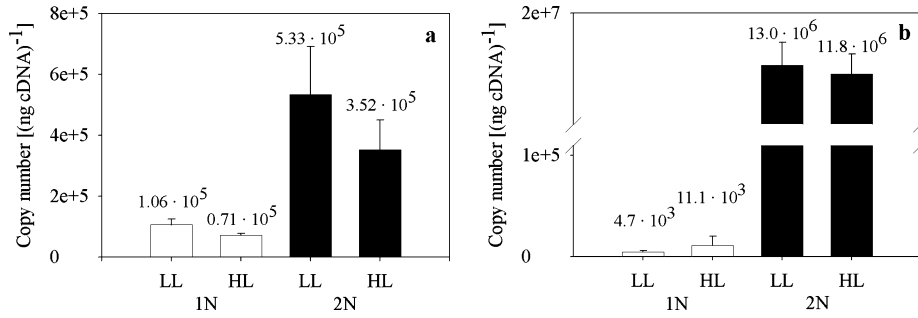


FIG. 3. Abundances of transcript copies of genes AP2B1 (a) and ATPVa (b) in haploid (1N) and diploid (2N) *Emiliania huxleyi* cells acclimated to low light (LL) and high light (HL) intensities.

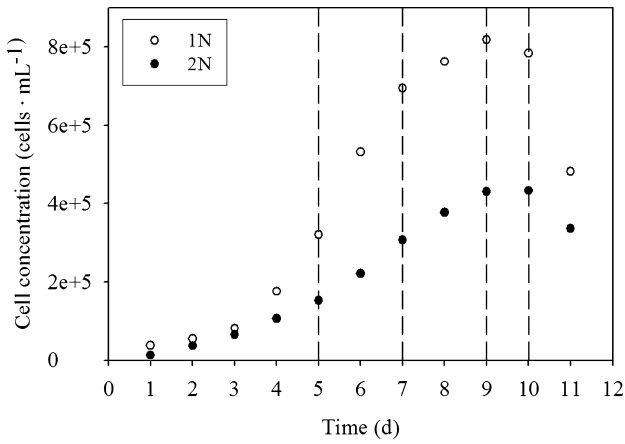


FIG. 4. Time course of culture growth for microbead treatment; dashed lines indicate samplings.

necessary genes, absence of the phenotypic ability must be attributed to suppression of gene transcription in the diplont. The presence of these pathways in the haploid stage, however, may indicate a stage-specific constitutive expression.

Higher expression of cytoskeleton-related genes in the haploid stage must be attributed to the fact that this stage is flagellated (von Dassow et al. 2009). Tubulins and their associated motors are crucial for cell motility, a trait specific to the haploid stage. Diploid cells may only express the amounts of transcripts needed for maintenance of intracellular microtubular structures.

The haploid *E. huxleyi* stage exhibits a pronounced carboxylic acid and energy metabolism (malate dehydrogenase, pyruvate carboxylase, and F₀F₁-ATP-Synthase subunits). The expression of isocitrate lyase was increased. This enzyme, catalyzing

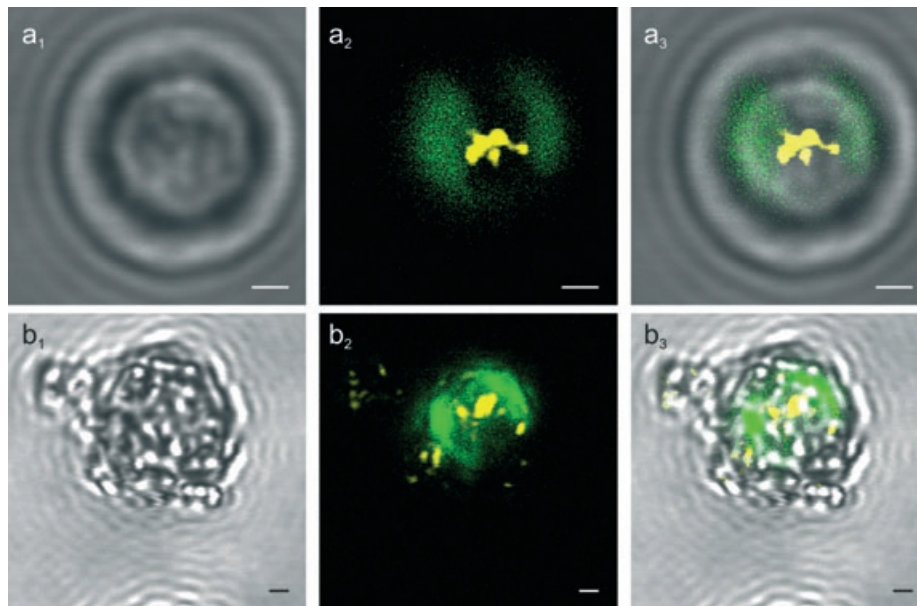


FIG. 5. Ingested fluorescent beads in haploid (a) and diploid (b) individuals of *Emiliania huxleyi*: 1, transmission image of single cells; 2, combined fluorescent scans indicating the respective cellular localization of the beads (yellow, emission 500–560 nm) and the chloroplasts (green, emission 610–670 nm); 3, confocal scans superimposed on transmission image (1 + 2). Scale bar = 1 μm.

the conversion of isocitrate into succinate and glyoxylate and vice versa, is able to convey catabolically produced C_2 products (e.g., from digestion of lipids) into anabolic C_3/C_4 carboxylic acid metabolism. This finding suggests a broad flexibility with respect to regulation of co-occurring anabolic and catabolic activities and resource management.

The elevated expression of GPA is in agreement with the findings of von Dassow et al. (2009). This protein was hypothesized to assist in the nucleation of calcium carbonate crystals (Corstjens et al. 1998). The increased expression indicates that GPA obviously fulfills cell-biological tasks in the noncalcifying life-cycle stage as well. As it was discussed to be associated with secretory polysaccharides, von Dassow et al. (2009) argued that it might also be involved in the formation of the extracellular organic scales observed in this life-cycle stage.

DNA sequence variations within the GPA gene were successfully used as a molecular marker within the species *E. huxleyi* (Schroeder et al. 2005), being able to tell apart A and B coccolith morphotypes. The detection of the mRNA of the strain used in this study (R morphotype) must therefore be attributed to the unspecificity of the oligonucleotide probe used toward minor sequence differences. Sequencing of the GPA transcript of strain 1216/1217 may be performed to validate the functionality of this genetic marker and possibly extend its usage to this and other R morphotype strains.

The haploid-specific transcriptome further displays a prominent increase in features related to ubiquitin-mediated proteasomal degradation, the process in which proteins are selectively disassembled into amino acids. As argued by Klaveness (1972), mechanical stress (e.g., by aerating the culture) may rupture the flagellae and impair the cells' physiology. In microscopic examinations, however, cells were intact and actively swimming, and growth rates were consistently high. The increased expression of ubiquitin-related machinery may rather be linked to the relatively intense catabolic activity and nitrogen metabolism discussed above and might therefore indicate higher relative protein turnover, which could increase the flexibility of the proteome to respond more quickly to short-term cellular demands.

Diplont-specific transcriptome. In the diplont, increased expression of genes involved in chromatin structuring, like Pob3 homologs (Formosa et al. 2001) and DNA methyl- and acetyltransferases (Bird 2002), must be linked to the epigenetic management of the double set of chromosomes. As in all diploid organisms, cells need to suppress transcription of double alleles to avoid futility and possibly adverse gene-dosage effects (Papp et al. 2003). Apparent absence of vitamin-synthesizing gene products in the diploid stages of some *E. huxleyi* strains may be attributed to such selective gene-silencing. Diploid cells also strongly express machinery related

to pre-mRNA modifications, that is, differential splicing (Blencowe et al. 2000), which might increase the versatility of the proteome on a post-transcriptional basis.

Transcripts related to PKSs were detected in higher amounts in diploid *E. huxleyi*. These evolutionary deep-branching enzymes synthesize a broad range of long-chained secondary metabolites, which can be relevant in species interactions such as defense or hunting (John et al. 2008 and references therein). Given the modular structure of PKSs, the observed transcripts cannot be attributed to any particular chemical and thus their function in *E. huxleyi* requires further investigations. These enzymes might, however, potentially be related to polyunsaturated long-chain (C_{37-39}) alkenones, alkenoates, and alkenes (Eltgroth et al. 2005), which have been extensively studied as biomarkers and paleo-proxies (Beltran et al. 2007).

The prominent expression of V-ATPase subunits in diploid cells indicates a higher activity of the EMS, in particular the maintenance of vacuolar membrane potentials and proton gradients. Acidification of vacuolar compartments plays a key role in multiple cellular processes including endocytosis, macromolecular processing and degradation, as well as coupled transport of small molecules (Stevens and Forgac 1997). In the coccolithophore *Pleurochrysis carterae*, a dedicated V-ATPase, mediating H^+ -transport in a Ca^{2+} -dependent manner, was found in coccolith vesicles (Corstjens and Gonzáles 2004). Thus, high relative expression of V-ATPase, which was also confirmed in the diplont by qRT-PCR (>1,000-fold expression relative to the noncalcifying haploid stage), is likely to be linked to coccolithogenesis. Although seemingly counterintuitive, an inward proton pumping is suspected to play a major role in the complex acid-base chemistry of coccolith-producing vesicles (Mackinder et al. 2010). Vacuolar H^+ -ATPases that energize transporter-mediated alkalization of the extracellular space have been observed, and mechanistic models have been proposed by which pH-coupled ion-transport may achieve this (Harvey 2009).

Furthermore, increased expression levels of the CAX3 Ca^{2+}/H^+ antiporter and of a Cl^-/HCO_3^- exchanger of the SLC4 family were observed. These gene products have been observed to be expressed specifically in the diplont (von Dassow et al. 2009) and were postulated to play active roles in coccolithophore biomineralization (Mackinder et al. 2010). With respect to the EMS, diploid *E. huxleyi* are significantly richer in gene transcripts related to formation and traffic of endocytotic clathrin-coated vesicles, especially AP2-related subunits. The coexpression of machinery involved in endocytosis and endosomal vesicle sorting, like SNARE type sorting factors (von Dassow et al. 2009) suggests higher endocytotic activity in the diploid stage. Increased retrograde membrane traffic is a cell-biological

necessity in this stage, as the continuous export of coccoliths by exocytosis would otherwise eventually diminish the EMS. Interestingly, a versatile set of proteases, many of which are putative zymogen-activating enzymes, were also observed to be up-regulated in the diploid transcriptome. These vesicular proteases are known to cleave enzyme precursors to enable their activity, often for degradative purposes. This finding might be interpreted as a sign of increased secretion of degrading enzymes to vesicles or the extracellular space. Yet, a significant fraction of these proteases cannot be assigned to pro-protein conversion due to their exopeptidase character. These enzymes participate in proteolytic degradation within digestive compartments. They might serve the recycling of retrieved membrane proteins but also represent the basic machinery needed for the digestion of endocytosed extracellular matter.

Data indicate that haploid cells drive a flexible conventional primary metabolism involving classical anabolic and catabolic key pathways and increased protein turnover. The smaller genome of the haploid stage and hence the more parsimonious and basic transcriptome simplify the processes of gene expression and thereby minimize cellular energetic and material efforts. As the haploid stage is thought to occur mainly as an “ecological backup” of the terminated diploid population, its higher initial numbers and the streamlined metabolism may lead to high competitiveness and enable it to thrive in postbloom waters.

The diploid stage, in turn, strongly expresses machinery related to epigenetic management of chromosomes and pretranslational processing of mRNA. Together with pronounced expression of transcriptional regulation machinery, these findings indicate that the versatility of the diploid proteome is controlled more on a pretranslational basis, rather than by posttranslational modifications and increased protein turnover as observed in the haploid stage.

E. huxleyi: a mixotrophic phytoplankton species? Most haptophytes possess chloroplasts and are therefore considered photoautotrophs. Some species (e.g., *Prymnesium parvum*) have, however, been shown to be capable of ingesting dissolved or particulate organic material (Jones et al. 1994, Tillmann 2003). The motility and reduction of calcification in the haploid stage of *E. huxleyi* have been hypothetically linked to mixotrophic behavior (Houdan et al. 2005).

The transcriptome analyses indicated endocytotic activity in the exponential growth phase, whereas the microscopy observations revealed phagocytotic particle uptake only in late stationary phase. This emphasizes the critical difference between constitutive endocytotic activity as a vital cellular function and an inducible phagocytotic particle uptake. It further indicates that phagocytotic behavior is induced only under certain environmental conditions, for

example (post-) bloom settings with depleted macro- and/or micronutrients. Yet, the particular triggers and purposes of phagotrophy in *E. huxleyi* remain elusive.

Recent research indicates, however, that endocytotic vesicles might be the vehicle exploited in viral infection of diploid *E. huxleyi* cells (Mackinder et al. 2009). It may therefore be hypothesized that under limiting (i.e., bloom-) conditions, the virus hitchhikes the induced phagocytotic machinery to intrude cells and induce bloom termination. Clearly, more research is necessary to elucidate the interconnections between environmental conditions, ecological succession scenarios, and life cycling in *E. huxleyi*, in which the reasons for the high competitiveness of this species in contemporary oceans might lie.

This work was supported by the European Research Council under the European Community's Seventh Framework Programme (FP7/2007-2013)/ERC grant agreement no. [205150] and by the project BOOM (Biodiversity of Open Ocean Microcalcifiers), funded by the Institut Français de la Biodiversité via the Agence National de la Recherche, grant ANR-05-BDIV-004. L. J. d. N. is supported through the European Project on Ocean Acidification (EPOCA) and the program on Biological Impacts of Ocean Acidification (BIOACID). The *E. huxleyi* draft genome was provided by JGI, which is supported by the Office of Science of the U.S. Department of Energy under contract no. DE-AC02-05CH11231. We like to thank Sylke Wohlrab for assistance in microarray hybridizations and evaluation as well as Ian Probert for providing cultures of *E. huxleyi*. Further, we thank Peter von Dassow, Gerald Langer, Sven Kranz, Urban Tillmann, and Mirko Lunau for productive discussions. We also thank Daniel Vaultot and two anonymous reviewers for their thorough and productive criticism that helped to shape the manuscript.

- Beltran, C., de Raféls, M., Minoletti, F., Renard, M., Sicra, M. A. & Ezat, U. 2007. Coccolith $\delta^{18}\text{O}$ and alkenone records in middle Pliocene orbitally controlled deposits: high-frequency temperature and salinity variations of sea surface water. *Geochem. Geophys. Geosyst.* 8:Q05003. DOI: 10.1029/2006GC001483.
- Billard, C. 1994. Life cycles. In Green, J. C. & Leadbeater, B. S. C. [Eds.] *The Haptophyte Algae*. Clarendon Press, Oxford, UK, pp. 167–86.
- Bird, A. 2002. DNA methylation patterns and epigenetic memory. *Genes Dev.* 16:6–21.
- Blencowe, B. J., Baurén, G., Eldridge, A. G., Issner, R., Nickerson, J. A., Rosonina, E. & Sharp, P. A. 2000. The SRm160/300 splicing coactivator subunits. *RNA* 6:111–20.
- Bratbak, G., Wilson, W. & Heldal, M. 1996. Viral control of *Emiliania huxleyi* blooms? *J. Mar. Syst.* 9:75–81.
- Corstjens, P. L. A. M. & Gonzáles, E. L. 2004. Effects of nitrogen and phosphorus availability on the expression of the coccolith-vesicle V-ATPase (subunit c) of *Pleurochrysis* (Haptophyta). *J. Phycol.* 40:82–7.
- Corstjens, P. L. A. M., van der Kooij, A., Linschooten, C., Brouwers, G. J., Westbroek, P. & de Vrind-de Jong, E. 1998. GPA, a calcium-binding protein in the coccolithophorid *Emiliania huxleyi* (Prymnesiophyceae). *J. Phycol.* 34:622–30.
- von Dassow, P., Ogata, H., Probert, I., Wincker, P., Da Silva, C., Audic, S., Claverie, J. M. & de Vargas, C. 2009. Transcriptome analysis of functional differentiation between haploid and diploid cells of *Emiliania huxleyi*, a globally significant photosynthetic calcifying cell. *Gen. Biol.* 10:R114. DOI: 10.1186/gb-2009-10-10-r114.

- Dickson, A. G. 1990. Standard potential of the reaction: $\text{AgCl(s)} + \frac{1}{2} \text{H}_2(\text{g}) = \text{Ag(s)} + \text{HCl(aq)}$, and the standard acidity constant of the ion HSO_4^- in synthetic seawater from 273.15 to 318.15 K. *J. Chem. Thermodynamics* 22:113–27.
- Dickson, A. G. & Millero, F. J. 1987. A comparison of the equilibrium constants for the dissociation of carbonic acid in seawater media. *Deep-Sea Res.* 34:1733–43.
- Eltgroth, M. L., Watwood, R. L. & Wolfe, G. V. 2005. Production and cellular localization of neutral long-chain lipids in the haptophyte algae *Isochrysis galbana* and *Emiliania huxleyi*. *J. Phycol.* 41:1000–9.
- Falkowski, P. G. & Raven, J. A. 2007. *Aquatic Photosynthesis*, 2nd ed. Princeton University press, Princeton, New Jersey, pp. 1–3.
- Formosa, T., Eriksson, P., Wittmeyer, J., Ginn, J., Yu, Y. & Stillman, D. J. 2001. Spt16-Pob3 and the HMG protein Nhp6 combine to form the nucleosome-binding factor SPN. *EMBO J.* 20:3506–17.
- Frada, M., Probert, I., Allen, M. J., Wilson, W. H. & De Vargas, C. 2008. The “Cheshire Cat” escape strategy of the coccolithophore *Emiliania huxleyi* in response to viral infection. *Proc. Natl. Acad. Sci. U. S. A.* 105:15944–9.
- Green, J. C., Course, P. A. & Tarran, G. A. 1996. The life-cycle of *Emiliania huxleyi*: a brief review and a study of relative ploidy levels using flow cytometry. *J. Mar. Syst.* 9:33–44.
- Guillard, R. R. L. & Ryther, J. H. 1962. Studies of marine planktonic diatoms. *Can. J. Microbiol.* 8:229–39.
- Harvey, W. R. 2009. Voltage coupling of primary H^+ V-ATPases to secondary Na^+ - or K^+ -dependent transporters. *J. Exp. Biol.* 212:1620–9.
- Houdan, A., Véron, B., Claquin, P., Lefebvre, S. & Poncet, J. M. 2005. Cryopreservation of the coccolithophore *Emiliania huxleyi* (Haptophyta, Prymnesiophyceae). *J. Appl. Phycol.* 17:413–22.
- John, U., Beszteri, B., Derelle, E., de Peer, Y. V., Read, B., Moreau, H. & Cembella, A. 2008. Novel insights into evolution of protistan polyketide synthases through phylogenomic analysis. *Protist* 159:21–30.
- Jones, H. L. J., Leadbeater, B. S. C. & Green, J. C. 1994. Mixotrophy in haptophytes. In Green, J. C. & Leadbeater, B. S. C. [Eds.] *The Haptophyte Algae*. Clarendon Press, Oxford, UK, pp. 167–86.
- Klavness, D. 1972. *Coccolithus huxleyi* (Lohm.) Kamptn. II. The flagellate cell, aberrant cell types, vegetative propagation and life cycles. *Br. Phycol. J.* 7:309–18.
- Krell, A., Funck, D., Plettner, I., John, U. & Dieckmann, G. 2007. Regulation of proline metabolism under salt stress in the psychrophilic diatom *Fragilariopsis cylindrus* (Bacillariophyceae). *J. Phycol.* 43:753–62.
- Legrand, C. & Carlsson, P. 1998. Uptake of high molecular weight dextran by the dinoflagellate *Alexandrium catenella*. *Aquat. Microb. Ecol.* 16:81–6.
- Lewis, E. & Wallace, D. W. R. 1998. *Program Developed for CO₂ System Calculations*. Carbon Dioxide Information Analysis Centre, Oak Ridge National Laboratory, U.S. Department of Energy, Oak Ridge, Tennessee.
- Livak, K. J. & Schmittgen, T. D. 2001. Analysis of relative gene expression data using real-time quantitative PCR and the 2- $^{-\Delta\Delta\text{CT}}$ method. *Methods* 25:402–8.
- Mackinder, L. C. M., Wheeler, G. L., Schroeder, D. C., Riebesell, U. & Brownlee, C. 2010. Molecular mechanisms underlying calcification in coccolithophores. *Geomicrobiol. J.* 27:585–95.
- Mackinder, L. C. M., Worthy, C. A., Biggi, G., Hall, M., Ryan, K. P., Varsani, A., Harper, G. M., Wilson, W. H., Brownlee, C. & Schroeder, D. C. 2009. A unicellular algal virus, *Emiliania huxleyi* virus 86, exploits an animal-like infection strategy. *J. Gen. Virol.* 90:2306–16.
- Mehrbach, C., Culbertson, C. H., Hawley, J. E. & Pytkowicz, R. M. 1973. Measurement of the apparent dissociation constants of carbonic acid in seawater at atmospheric pressure. *Limnol. Oceanogr.* 18:897–907.
- Mohan, R., Mergulhao, L. P., Guptha, M. V. S., Rajakumar, A., Thamban, M., Anil-Kumar, N., Sudhakar, M. & Ravindra, R. 2008. Ecology of coccolithophores in the Indian sector of the Southern Ocean. *Mar. Micropaleontol.* 67:30–45.
- Papp, B., Pal, C. & Hurst, L. D. 2003. Dosage sensitivity and the evolution of gene families in yeast. *Nature* 424:194–7.
- Provasoli, L. & Carlucci, A. F. 1974. Vitamins and growth regulators. In Stewart, W. D. P. & Pierce, C. E. [Eds.] *Algal Physiology and Biochemistry*. Blackwell, Malden, Massachusetts, 741 pp.
- Raven, J. A. 1997. Phagotrophy in phototrophs. *Limnol. Oceanogr.* 42:198–205.
- Rost, B. & Riebesell, U. 2004. Coccolithophores and the biological pump: responses to environmental changes. In Thierstein, R. & Young, J. R. [Eds.] *Coccolithophores: From Molecular Processes to Global Impact*. Springer-Verlag, Berlin, pp. 99–125.
- Rozen, S. & Skaletsky, H. J. 2000. Primer3 on the WWW for general users and for biologist programmers. In Krawetz, S. & Misener, S. [Eds.] *Bioinformatics Methods and Protocols: Methods in Molecular Biology*. Humana Press, Totowa, New Jersey, pp. 365–86.
- Saeed, A. I., Sharov, V., White, J., Li, J., Liang, W., Bhagabati, N., Braisted, J., Klapa, M., Currier, T. & Thiagarajan, M. 2003. TM4: a free, open source system for microarray data management and analysis. *BioTechniques* 34:374–8.
- Schroeder, D. C., Biggi, G. F., Hall, M., Davy, J., Martinez, J., Richardson, A. J., Malin, G. & Wilson, W. H. 2005. A genetic marker to separate *Emiliania huxleyi* (Prymnesiophyceae) morphotypes. *J. Phycol.* 41:874–9.
- Schroeder, D. C., Oke, J., Hall, M., Malin, G. & Wilson, W. 2003. Virus succession observed during an *Emiliania huxleyi* bloom. *Appl. Environ. Microbiol.* 69:367–79.
- Stevens, T. H. & Forgac, M. 1997. Structure, function and regulation of the vacuolar (H^+)-ATPase. *Annu. Rev. Cell Dev. Biol.* 13:779–808.
- Storey, J. D. 2003. The positive false discovery rate: a Bayesian interpretation and the q-value. *Ann. Stat.* 31:2013–35.
- Tillmann, U. 2003. Kill and eat your predator: a winning strategy of the planktonic flagellate *Prymnesium parvum*. *Aquat. Microb. Ecol.* 32:73–84.
- Tusher, V. G., Tibshirani, R. & Chu, G. 2001. Significance analysis of microarrays applied to the ionizing radiation response. *Proc. Natl. Acad. Sci. U. S. A.* 98:5116–21.
- Westbroek, P., Brown, C. W., Van Bleijswijk, J., Brownlee, C., Brummer, G. J., Conte, M., Egge, J. et al. 1993. A model system approach to biological climate forcing: the example of *Emiliania huxleyi*. *Glob. Planet. Change* 8:27–46.
- Winter, A., Jordan, R. W. & Roth, P. H. 1994. Biogeography of living coccolithophores in ocean waters. In Winter, A. & Siesser, W. G. [Eds.] *Coccolithophores*. Cambridge University Press, Cambridge, UK, pp. 161–77.

Supplementary Material

The following supplementary material is available for this article:

Table S1. Quantitative real-time polymerase chain reaction (qRT-PCR) primer sets for validated transcripts and the respective amplification efficiencies; MA and NSP data taken from Krell et al. (2007).

Table S2. Microarray data set of genes that are significantly up-regulated preferentially in the haploid (1N) and diploid (2N) stage.

This material is available as part of the online article.

Please note: Wiley-Blackwell are not responsible for the content or functionality of any supplementary materials supplied by the authors. Any queries (other than missing material) should be directed to the corresponding author for the article.